An Evolutionary Computational Framework for Capacity-Safety Trade-off in an Air Transportation Network

Md Murad Hossain, Sameer Alam, Daniel Delahaye

An Evolutionary Computational Framework for Capacity-Safety Trade-off in an Air Transportation Network

Md. Murad Hossain[a], Sameer Alam[b], Daniel Delahaye[c]

[a]*School of Engineering and Information Technology, University of New South Wales, Canberra, Australia*
[b]*School of Mechanical and Aerospace Engineering, Nanyang Technological University, Singapore*
[c]*MAIAA Laboratory, Ecole Nationale de l'Aviation Civile, Toulouse, France*

Abstract

Airspace safety and airport capacity are two key challenges to sustain the growth in Air Transportation. In this paper, we model the Air Transportation Network as two sub-networks of airspace and airports, such that the safety and capacity of the overall Air Transportation network emerge from the interaction between the two. We propose a safety-capacity trade-off approach, using a computational framework, where the two networks can interact and the trade-off between capacity and safety in an Air Transport Network can be established. The framework comprise of a Evolutionary Computation based air traffic scenario generation using a Flow Capacity Estimation Module (for capacity), Collision Risk Estimation module (for safety) and an Air Traffic Simulation module (for evaluation). The proposed methodology to evolve air traffic scenarios such that it minimizes collision risk for given capacity estimation was tested on two different air transport network topologies (random and small-world) with the same number of airports. Experimental results indicate that though airspace collision risk increases almost linearly with the increasing flow (flow intensity) in the corresponding airport network, the critical flow depend on the underlying network configuration. It was also found that, in general, the capacity upper bound depends not only on the

Email addresses: md.hossain@adfa.edu.au (Md. Murad Hossain), sameeralam@ntu.edu.sg (Sameer Alam), delahaye@recherche.enac.fr (Daniel Delahaye)

connectivity among airports and their individual performances but also the configuration of waypoints and mid-air interactions among fights. Results also show that airport network can accommodate more traffic in terms of capacity but the corresponding airspace network can not accommodate the resulting traffic flow due to the bounds on collision risk.

Keywords: Airport Network, Airspace Capacity, Collision Risk, Safety

1. Introduction

Air Transportation Network (ATN) is a complex system of systems which operates on the edge of chaos. It comprises of airports, airspace, air traffic control and CNS (Communication, Navigation and Surveillance) systems which work in tandem to achieve an orderly and safe flow of air traffic. Continuous growth in air traffic worldwide and the projected growth in air traffic demand[33, 27], coupled with the uncertainties arising in the system from weather, congestions, breakdowns, and other exogenous variables, brings new challenges and open research question on safety and capacity in an ATN. Air navigation service providers (ANSPs), universities and research organizations are exploring new paradigms (e.g. SESAR [13] and NextGen [30]) and innovative procedures (Dynamic Sectorization [7], Automated Separation Assurance [25], Performance Based Navigation (PBN) [28]) to accommodate growth while maintaining the overall safety of the ATN.

Recent research has highlighted the fact that the overall performance of an ATN is influenced by the interaction between two sub-networks: a network of airports and network of airspace [11, 37]. Since airports are the source and sink in an ATN, the airport network is constrained by capacity. Whereas, the airspace network is constrained by safety, measured by risk of collision against the Target Level of Safety (TLS) as defined by the International Civil Aviation Organization [19]. There are several initiatives to increase the capacity of the airport network and safety of the airspace network. For airports network, the capacity improvement efforts are mainly through better management of demand and supply (thus reducing delays) [20], traffic scheduling [32] and by better utilization of the regional airports around a major airports (hub-spoke) [1]. For airspace network safety improvement, they are mainly through collision risk modelling [3] and innovative airspace procedures (sectorization)[22]. However, how the two networks interacts with each other and influences each other in an ATN is not fully understood [39, 14].

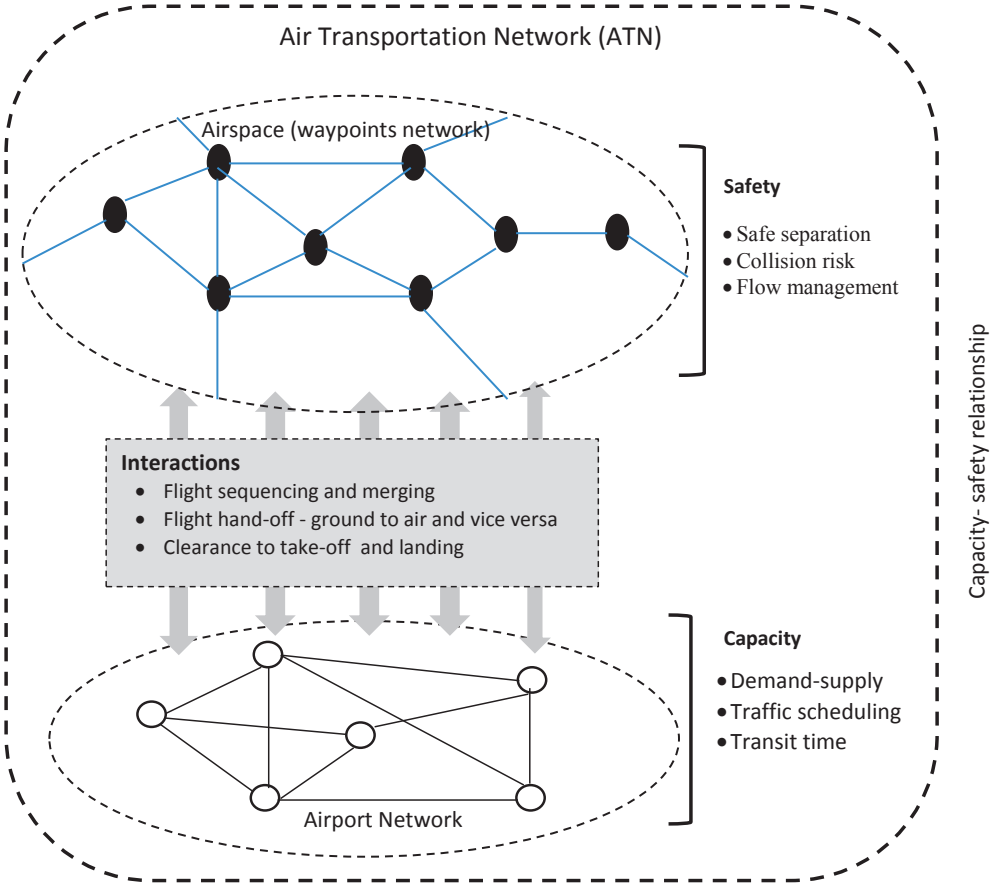

Figure 1: Interactions and constraints of airport and airspace network in an ATN

The concept of two networks interacting with each other in an ATN is further illustrated in Figure 1. It shows how the capacity and safety in an ATN may be influenced by the interactions and constraints of airport and airspace network in an ATN. Intuitively, as the aircraft density in a given volume of airspace or even in a whole ATN increases, without a change in control procedures, system safety will degrade as a result of more closely spaced operations [39]. So far, the relationship between the airport network in terms of capacity and airspace network in terms of safety in an ATN has not been investigated. A very limited literature exists on safety-capacity relationship in ATN, with most of the work focusing on individual element or components of an ATN [38, 39]. For example, Bojis et al. [38] investigated

the trade-off between the collision-risk and capacity of an en-route airspace, Haynie [14] looked into the relationship between capacity and safety in near-terminal airspace, Kopardekar et al. [23], investigated the capacity and safety in a sector and Pesic et al. [29]analysed the capacity-safety relationship for ground traffic movement at an airport.

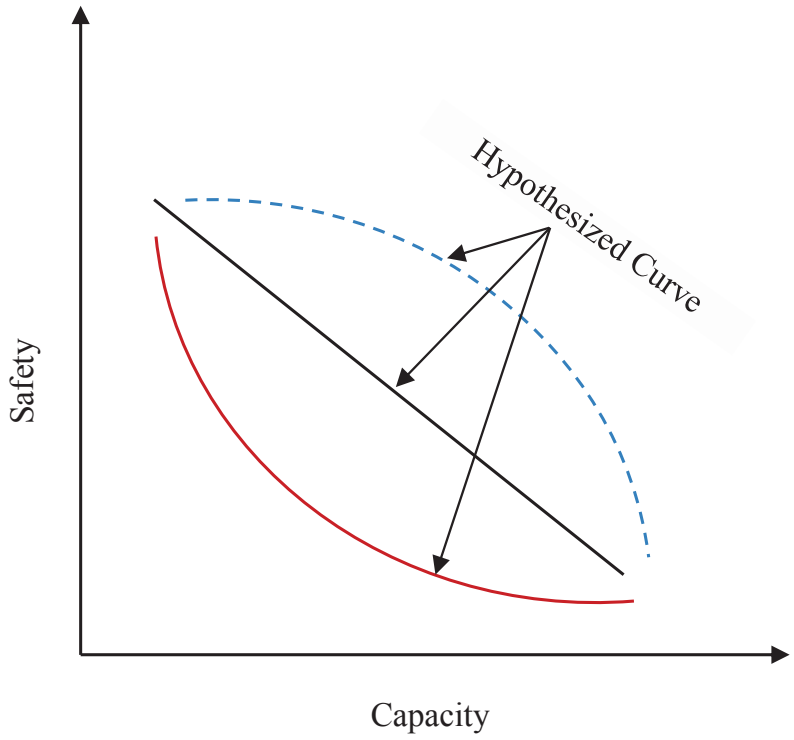

Figure 2: Hypothetical safety-capacity relationship curves

One way of expressing this relationship is by safety-capacity curves [39], with different possible trade-offs as shown in Figure 2. Identifying and understanding such relationship between capacity and safety of the two underlying networks is vital to improve the overall performance of an ATN. In this paper, we propose a computational framework for airport and airspace networks interaction in an ATN to analyse the trade-offs between airport network capacity and airspace network safety. The nodes in an airport network are the airports itself and the nodes in the airspace network are the airway-waypoints.

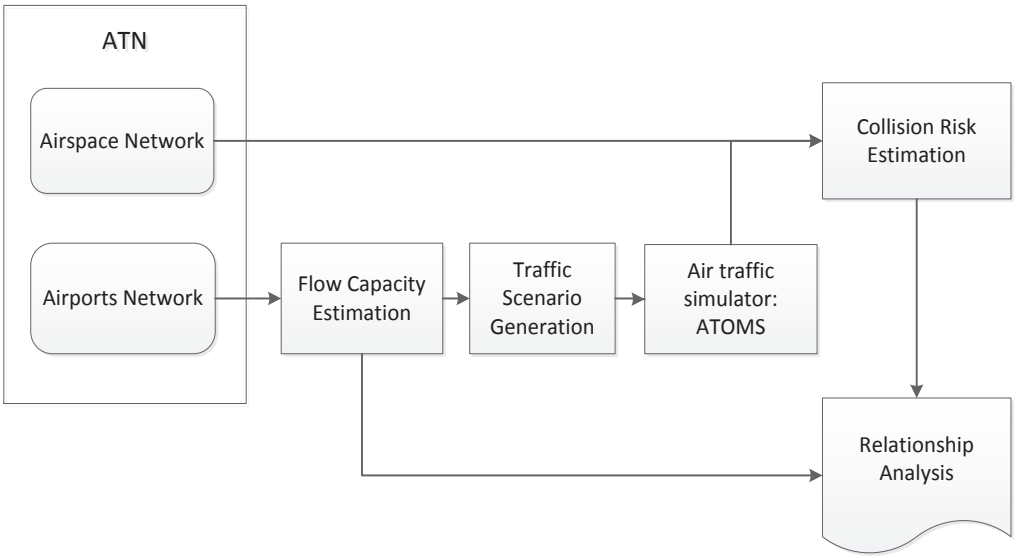

Figure 3: Conceptual approach for analysing capacity – collision risk relationship in an ATN

2. Proposed Approach

The proposed approach for analysing the capacity-safety relationship for an ATN is differs from safety assessment [34] and capacity estimation [8, 12] methods which, traditionally, have been modelled and evaluated independently. As illustrated in figure 3, for a given ATN, we first define its underlying airport and airspace network. Its capacity upper bound is estimated from the airport network using the capacity estimation model described in [15], which we called Flow Capacity Estimation Module. The output of the flow capacity estimation provides hourly flow densities (flight movements per hour) and a traffic schedule consisting of scheduled departure and arrival times for each flight. The output of the flow capacity estimation module are then converted into traffic scenarios by an Air Traffic Scenario Generation Module.

To generate traffic scenario(s) from a given traffic schedule such that it minimizes the risk of collision (thereby airspace safety) is highly challenging [5]. The large search space (possibilities) of traffic features and non-linear interactions among collision risk parameters, makes traditional search methods such as Monte Carlo unsuitable for this kind of problem [40]. We applied

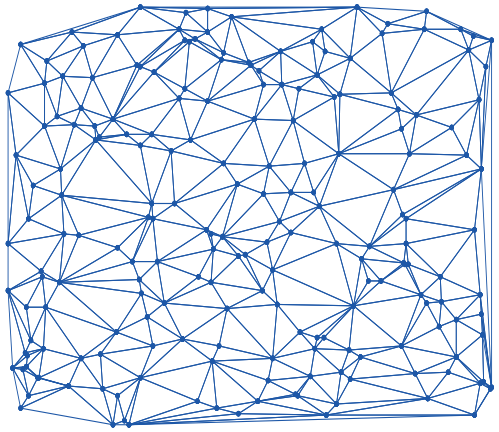

Figure 4: Example of Delaunay triangulation network

a population-based search technique known as Differential Evolution (DE) [31] to generate traffic scenario from the Flow Capacity Estimation Module. These traffic scenarios are then simulated in a high-fidelity air traffic simulator 'ATOMS' [2] which evaluates each scenario on risk of collision. Using the feedback from ATOMS, Differential Evolution allows us to further generate (evolve) the traffic scenarios which minimizes the collision risk. For Collision Risk assessment we use $1.5 \times 10^{-}8$ collision per flight hour as target level of safety [19]. The Collision Risk model is incorporated in to ATOMS which estimates the collision risk of a given traffic scenario and act as driving mechanism for further evolution (using DE) of traffic scenarios. This allows us to investigate the capacity-safety relationship curves for different traffic scenarios.

3. Air Transportation Network Model

An ATN is a composite network of airports and airspaces, where airports are linked through airspaces, comprising of a airways-waypoints on which the air traffic flows, is modelled as a time space network [16, 35, 21]. In the space-domain, the height is ignored and the ATN is embedded in a two-dimensional Euclidean space, i.e., the nodes (airports and waypoints) are associated with a stationary geographical location [21]. Since the objective of this paper is to investigate the relationship between two major sub-networks of an ATN, we model it accordingly.

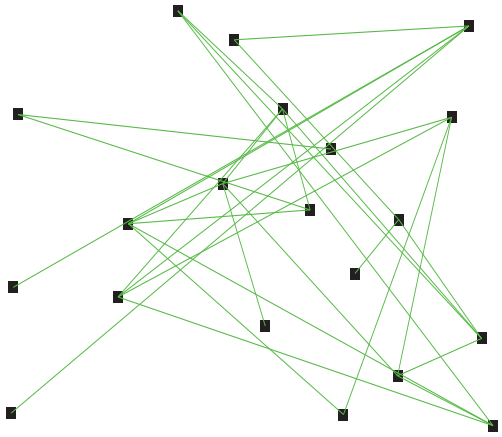

Figure 5: Random airport network configuration generated from Delaunay triangulation point set (Q)

3.1. Network Generation

An ATN can be generated in two different ways (i) generate a network with two different type of nodes airports and waypoints and (ii) generate the airport network and airspace network separately and then combine them togethers. Both of the approach will ended up to a similar ATN, as a result we have considered the first approach only. To generate it we extend the technique developed by Mehadhebi [26] that consists of the following steps.

- Firstly, a Delaunay triangulation network of Q points is created in a given area. In mathematics and computational geometry, a Delaunay triangulation for a set (Q) of points in a plane is a triangulation ($DT(Q)$) such that no point in Q is inside the circumference of any triangle in $DT(Q)$. we apply the Delaunay triangulation algorithm [6] to create Q in a two-dimensional plan with no overlapping connections among the points, each of which is an associated value of its latitude and longitude, to define its geographical location. Figure 4 shows a Delaunay triangulation network of $Q = 500$ points in an area of 200 square nautical miles.

- As, in a Delaunay triangulation network, some of the points tend to be very close to each other, we merge all the intersecting points that are too close. Although this will, in some way, increase the overall route distances, its benefit is reduced complexity of the ATN.

- As we define an ATN as a combination of an airport network and airspace network (network of waypoints), the next step is to create the underlying airport network. Let V be a set of airports chosen randomly from Q ($V \subset Q$) with the rest of the points (QV) defined as waypoints. The connections among the airports (V) are developed using complex network generation models (random graphs [10] and small-world networks [36]) to create the topology of the airport network. In it, the connected airports are separated by at least 100 nautical miles so that a flight spends at least 70% of its travel time in the cruise phase. Figure 5 presents an example of an airport network with 20 airports.

- Finally, the ATN is constructed by combining the shortest paths among the directly connected airports along the Delaunay triangulation network. Letting P be the set of shortest paths for all the connected airports in the airport network, the ATN is defined as:

$$ATN = \bigcup_{p_i \in P} p_i \tag{1}$$

  Figure 6 shows an ATN created from the Delaunay triangulation and airport network described in the above steps.

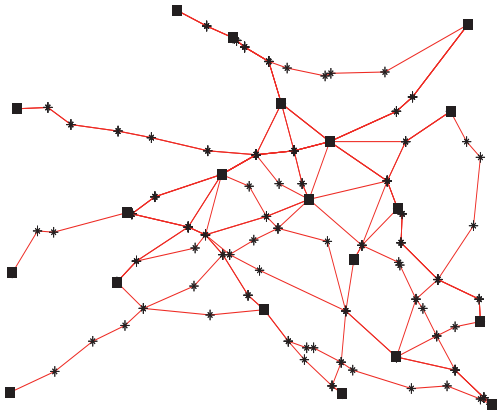

Figure 6: ATN of 20 airports (filled squares (■) represents present airports and stearics ($*$) waypoints)

4. Methodology

Having generated the ATN, the methodology for analysing the relationship between the airport network capacity and airspace network collision risk involves the following three key stages.

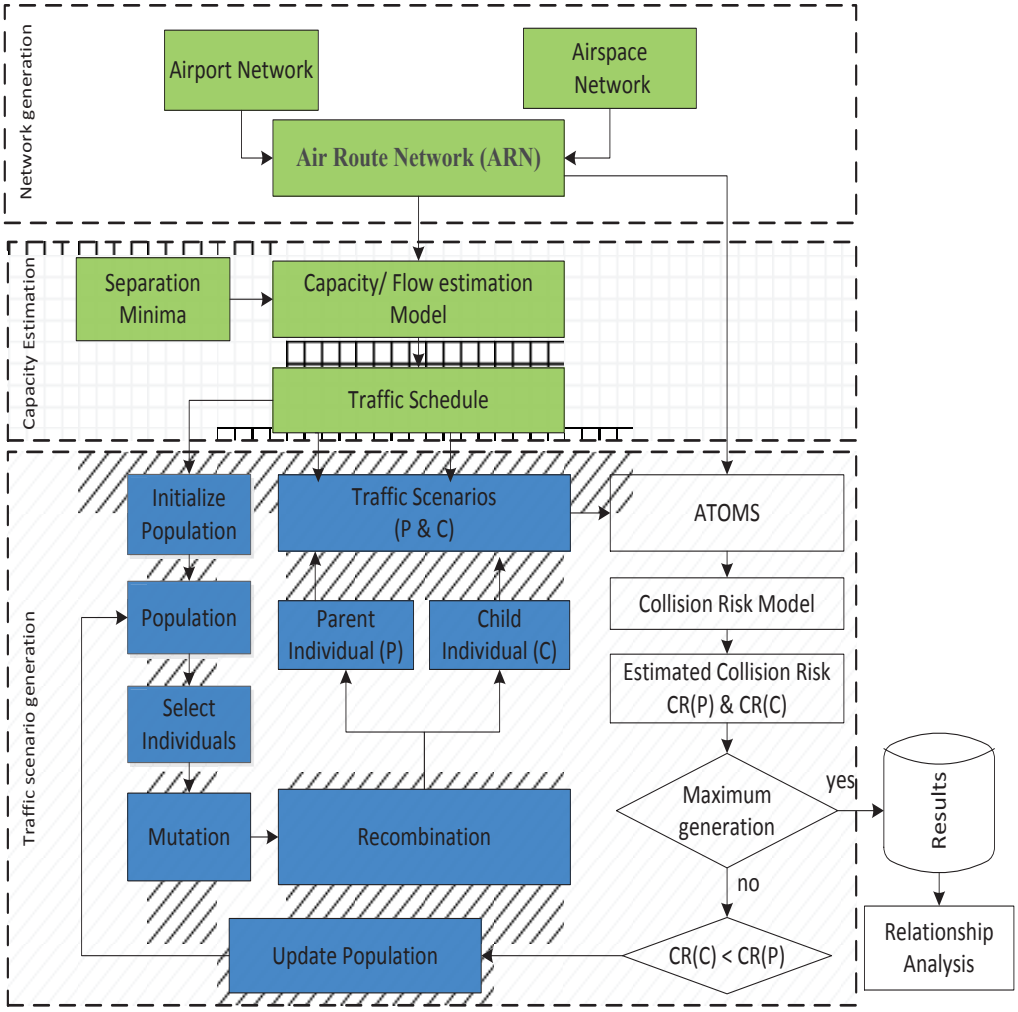

Figure 7: Evolutionary framework for analysing capacity-collision risk relationship in ATN

1. **Network Capacity Estimation:** the capacity of an ATN is defined as the maximum traffic that can be accommodated by its airport net-

work subject to resource constraints, such as fleet mix and node/link capacity, which determines the limit of feasible flow an air transportation network can accommodate. The flow intensity level is controlled by the wake-vortex separation minima, with an increase in the wake-vortex separation among aircraft during landing and take-off resulting in a decrease in the hourly flow in the ATN.

2. **Traffic Scenario Generation with Define Flow Intensity:** in this stage, given the flow, a complete traffic scenario is generated in a way that minimises the overall collision risk using evolutionary optimisation. In this paper we have used the term flow (flow intensity) and capacity interchangeably.
3. **Collision Risk Estimation**: In any airspace, collision risk (the probability of two aircraft colliding per flight hour) is one of the key safety indicators as defined by the ICAO [19]. Collision risk is usually compared against a threshold value defined by ICAO, called target level of safety (TLS), which provides a quantitative basis for judging the safety of operations in an airspace network [24]. The given traffic scenario is simulated in ATOMS to calculate the total number of flight hours and the probability of collision for each proximate pair of aircraft and, integrated with the Hsu model [17], the overall collision risk is estimated.

Figure 7, illustrates the process for analysing the trade-off between the flow capacity and collision risk of a given ATN. It begins with a very low flow intensity and, once a traffic scenario is generated, the overall collision risk for that scenario is estimated. Then, the flow is increased and the process continues until the flow level reaches the maximum capacity bound. Once all the possible scenarios for different flow levels are evaluated, the repository data is subsequently analysed to reveal the trade-off.

4.1. Network Capacity Estimation

Estimating capacity of an airport network system is a very hard combinatorial problem problem. A few number of attempts have been made to estimate the total capacity of an entire airport network system for any region or country [8, 9]. Authors in [15] proposed a mathematical formulation and a heuristic solution for estimating the capacity of a given airport considering different fleet mix and travel time. However, the model only consider a discrete travel time for all type of aircraft. In this paper we enhance the airport

network capacity estimate model to accommodate different travel time for different aircraft as follows:

Let, t_{ij}^{L}, t_{ij}^{M} and t_{ij}^{H} denote the required travel time from airport i to j by a light, medium and heavy aircraft respectively and $TD(f)$ and $TA(f)$ denote the time of departure (take-off) and time of arrival (landing) of a flight f from node i to j. Without loosing the general definition of travel time constraint define in [15], we can modify it as $TA(f) = TD(f) + d_f + t_{ij}^{x}$, where $x \in L, M, H$ is the type of aircraft of f . This modification will increase the number of variables in the problem formulation but will not increase the complexity of the heuristic solution approach as in [15].

In this paper, we have used a time based separation minimum between landing-landing, taking off - taking off, landing-taking-off or vice-versa to avoid the wake-vortex turbulence which is given in the following tables 1. In addition to that we also introduce some extra separation (es) between two consecutive aircrafts. The value to extra separation (es) will serve as a control parameter to decease the maximum hourly flow in the network, when the value of $es = 0$ the output of the capacity estimation module will provide the capacity upper bound (maximum attainable flow). The solution of an airport capacity will provide a list of flights and their schedule departure and arrival time, that we called a traffic schedule. This traffic schedule then converted into a traffic scenario by assigning flight level, speed at different phase using a differential evolutionary optimization method and a air traffic simulator.

4.2. Traffic Scenario Generation

Generating traffic scenarios using simple rules or hand scripting results very few alternatives from which it will be very hard to derive any conclusions. In this paper, we design a traffic scenarios generation method based on an airport network capacity estimation model [15] using an evolutionary framework. For a given traffic schedule, a complete traffic scenario must contain the tracks or air routes, feasible flight levels, and velocities and rates of climb and descent of different flight phases for all flights. Also, since the ATN is simultaneously shared by many aircrafts, the path of each and every aircraft needs to be conflict-free. Therefore, converting the output from the airport networks capacity module (traffic schedule) to a traffic scenario is a complex task, to handle which we develop the following evolutionary computation framework.

Table 1: Separation minima (in minutes) between aircrafts considered in this paper

Separation minima (arrival - departure)			
Leading Aircraft	Trailing aircraft		
	L	M	H
L	2	2	2
M	2	2	2
H	2	2	3
Separation minima (departure - arrival)			
Leading Aircraft	Trailing aircraft		
	L	M	H
L	2	2	2
M	2	2	2
H	2	2	3
Separation minima (arrival - arrival or departure-departure)			
Leading Aircraft	Trailing aircraft		
	L	M	H
L	2	2	2
M	3	2	3
H	3	2	3

4.2.1. Evolutionary Computation Framework Design

Given an ATN and schedule of departures and arrivals of N flights and their routes, the problem of generating a traffic scenario involves determining the flight path levels of N flights that minimise the overall mid-air collision risk. Due to large search space (possibilities) and non-linear interactions between different components of air transportation system, make traditional search methods, such as Monte Carlo, computationally infeasible [4]. Nature-Inspired techniques such as differential evolution (DE) algorithms have emerged as an important tool to effectively address complex problems in air transportation domain. Differential Evolution [31] is a stochastic, population-based optimization algorithm belonging to the class of Evolutionary Computation algorithms. Differential Evolution algorithms are highly effective in optimizing real valued parameter (traffic schedule in our case) and real valued function (minimize collision risk in our case). They are also highly effective in finding approximate solutions to global optimization problems (airspace collision risk in our case).

The proposed methodology for evolving flight level for each flight is illustrated in Figure 7. To define the flight, we have used the shortest path from the origin to destination in the ATN for each flight. If there is more than one shortest path, one of them is chosen randomly and the flight levels evolved

using a DE algorithm. In figure 7 green boxes depict the airport network's capacity estimations which generate a traffic schedule, white boxes represent the air traffic simulation which evaluates a given traffic data for collision risk in an airspace and blue boxes represent the DE [31] process to evolve optimal flight levels.

The DE process begins by defining the upper and lower bounds of the flight path levels for each flight. It then undergoes a random initialisation (within the bounds) of a population of solutions representing a set of vectors, where the size of each vector is equal to the number of aircraft defined by the traffic schedule. Each vector is considered a traffic scenario which is then simulated in ATOMS for its collision risk estimation, where the speeds of the flights in different stages are determined. After an initial evaluation, these vectors undergo mutation and recombination to generate two vectors we call the target and trial vectors which compete with each other. The one that minimises the collision risk for the given traffic data is admitted to the next generation and the process continues until the maximum number of generations is reached. Then, the best-performing solutions (vectors) are selected from the final population.

Representation of Flight Levels: since the objective of generating a traffic scenario is to evolve the right flight level for each and every flight for a given flight schedule, the flight level is encoded in a genetic inspired data structure (chromosome). Figure 8 illustrates a set of chromosomes that constitutes the flight population in which each chromosome represents a set

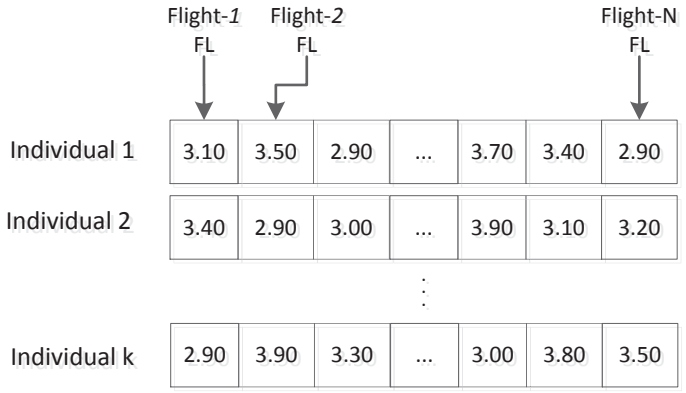

Figure 8: Chromosome design with encoded flight level (FL) for each flight in given traffic scenario

of flight levels to be applied to its corresponding flight; for example, if there are N flights, there will be N flight levels in a given chromosome. In this research, we do not consider semi-circular rules of flying and we choose only flight levels FL290 (29000ft) to FL-390 (39000ft) which are encoded as real values from 2.9 to 3.9 with a precession of 1, from which the actual flight levels are calculated using the equation $FL = (encoded\ value) \times 10000ft$.

Fitness Function: the role of a fitness function in an evolutionary algorithm (EA), Differential Evolution in our case, is to guide the search process by providing feedback on the quality of a solution represented by a chromosome in the population. Since this quality in our case depends on the estimated collision risk, we define the fitness as:

$$Fitness = min(collision\ risk) \tag{2}$$

Differential Evolution: to minimize the collision risk of a traffic scenario, we used a Differential Evolution optimization process. A DE starts with a population of M candidate solutions which is represented as $\vec{x}^{i}_{G=k} = \left[x^{i}_{1,k}, x^{i}_{2,k}, ..., X^{i}_{N,k}\right], i = 1, ..., M$, where N index denotes dimension of an individual, and G denotes the generation to which the population belongs.

In the initialization phase we define the upper and lower bounds for each chromosome value $L \leq x^{i}_{j,G=k} \leq U, \forall j$, where the lower bound is set to 2.90 and 3.90 respectively. We then randomly select the initial chromosome values uniformly in the intervals $[L, U]$. After the initialization, the effective evolution of DE depends on the manipulation and efficiency of three main operators; mutation, reproduction and selection. The DE algorithm applied in this paper is illustrated in algorithm 1.

5. Experimental Setup

In the experiments, we control the flow in the network by changing the extra separation parameter (es), starting with a low flow of es=20 and then gradually decreasing it by 1. For each es value, we generate 20 different traffic scenarios, each with the following parameter settings, using the evolutionary framework with different seeds and then estimate the collision risk.

- Test Network: in order to assess the effectiveness of the proposed airport network capacity estimation model, we perform experiments on two different types of test network: (i) ATN-I in which the airports and their connectivities are chosen randomly; and (ii) ATN-II in which

Algorithm 1 Traffic Scenario Generation

Let G denote a generation, P a population of size M, and $\vec{x}^{j}_{G=k}$ the j^{th} individual of dimension N in population P in generation k. cr is the crossover probability.
Input: $N, M > 4, F \in (0,1), cr \in (0,1)$
Initialize the population P
Each chromosome is a real valued vector
k=1
while (the stopping criterion is not satisfied or until maximum generation has reached) **do**
  j=0
  for $j \leq M$ **do**
    Randomly select $r_1, r_2, r_3 \in (1, ..., M), j \neq r_1 \neq r_2 \neq r_3$
    for $l \leq N$ **do**
      if $(random[0,1] < cr)$ **then**
        $x'_l = x^{r_3}_{l,G=k-1} + F \times (x^{r_1}_{l,G=k-1} - x^{r_2}_{l,G=k-1})$
      else
        $x'_l = x^{j}_{l,G=k-1}$
      end if
    end for
    $f(\vec{x}')$=evaluate $(\vec{x}')$
    $f(\vec{x}^{j}_{G=k-1})$=evaluate$(\vec{x}^{j}_{G=k-1})$
    if $f(\vec{x}') \leq f(\vec{x}^{j}_{G=k-1})$ **then**
      $\vec{x}^{j}_{G=k} = \vec{x}'$
    else
      $\vec{x}^{j}_{G=k} = \vec{x}^{j}_{G=k-1}$
    end if
  end for
  k=k+1
end while

the locations of the airports are placed on the circumference of a circle and their connectivities created using the small-world model [36]. Both these networks consist of 20 airports, as shown in Figure 9, with the difference between them their airport network topologies as ATN-I is considered a random and ATN-II a small-world network.

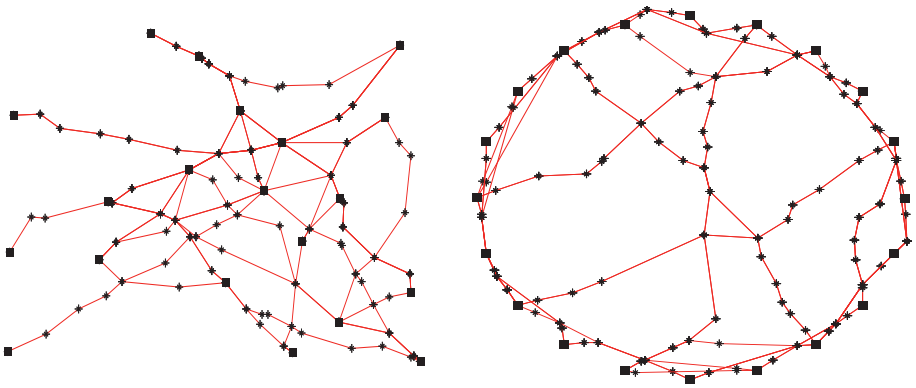

(a) Test ARN-I (b) Test ARN-II

Figure 9: Layout of test ATNs

Table 2: Diameters of cylinder (in metres) for different proximity pairs

Leading Aircraft	Trailing aircraft		
	L	M	H
L	140m	150m	180m
M	150m	192m	192m
H	180m	192m	220m

- Collision Risk Parameters: the Collision Risk models parameters are set as follows: Vertical overlap probability $P_z(0) = 0.55$, vertical speed when in horizontal flight $|\dot{z}| = 1.5m/s$ and aircraft position update time $T_{min} = 0.16$ minutes. The the diameter of aircraft cylinder (aircraft safety protection volume) is set based on the aircraft type of the proximity pair as shown in table 2, whereas, the height of the cylinder is set to$\lambda_z = 55m$ for all cases.

- Evolution Parameters: in our experiments, we use a population of 50 individuals and DE mutation factor (F) of 0.40. we conduct a series of experiments to determine the maximum number of generations for stopping and the proper crossover rate by running the evolution for up to 500 generations using different crossover rates. Figure 10 shows the best fitness values (minimum collision risks) of the population over generations from which it is clear that, after 350 generations, the best individual value does not improve in all cases. Therefore, as we can say

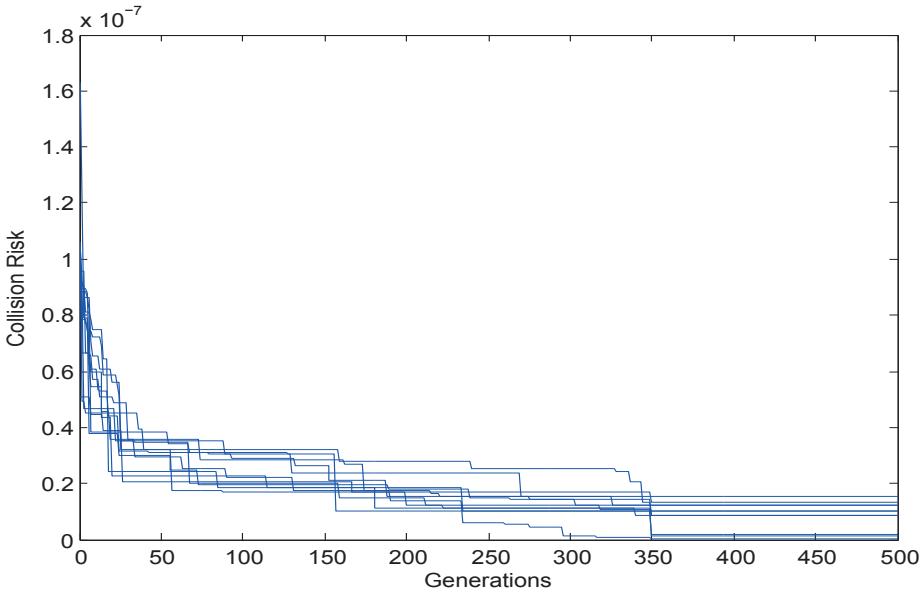

(a) Convergence of collision risk

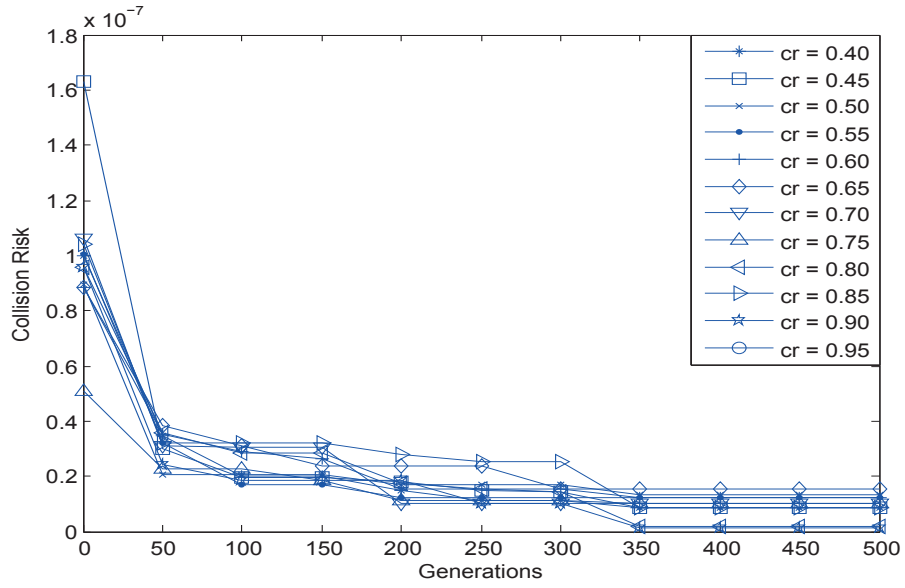

(b) Convergence of collision risk (discretisation after every 50 generation)

Figure 10: Selection of evolution parameter (maximum generation and crossover rate)

that 400 generations is sufficient to converge the evolution process, this is set as the stopping criterion for the DE process in the subsequent analysis.

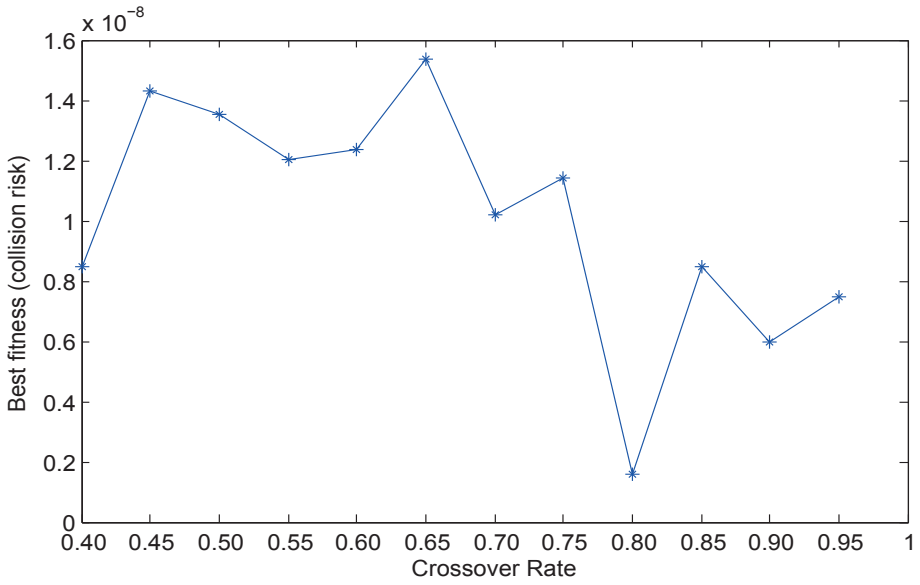

Figure 11: Best fitness values after final generation with different crossover rates (cr)

In order to determine a proper crossover rate, we perform experiments with different ones. Figure 11 shows the best fitness values after the final generation for different crossover rates (cr) ranging from 0.40 to 0.95 with an increment of 0.05 after 500 generations which indicates that the best fitness value is the lowest for a crossover rate of 0.80. Therefore, we set the crossover rate for DE to 0.80 for the subsequent analysis.

6. Results and Analysis

We first present the characterization of the test ARNs. In the test ATN-I, the underlying airport network has a uniform degree distribution, which is shown in table 3. In the ATN-II, the small-world topology of airport network is created with a staring ring lattice where every node is connected to its $K = 4$ neighbours ($K/2$ on either side), where K represent the mean degree

Table 3: Connectivity of the airports in ATN-I.

Node	Degree			Node	Degree		
	In	Out	Total		In	Out	Total
0	2	2	4	10	2	4	6
1	1	3	4	11	5	6	11
2	3	4	7	12	2	5	7
3	4	2	6	13	2	3	5
4	7	4	11	14	4	0	4
5	5	2	7	15	1	2	3
6	1	3	4	16	2	5	7
7	4	3	7	17	2	0	2
8	3	1	4	18	4	5	9
9	5	4	9	19	1	2	3

of the network, then it under goes a random rewiring with a probability of 0.05.

Apart from the connectivity pattern we also present the distance in nautical miles among the connected airports and number of way-points along the shortest path between them for ATN-I and ATN-II in Table 4 and Table 5 respectively. From table 4 and 5 it is clear that the minimum distance among the airport's links are $100.51NM$ and $101.59NM$ for ATN-I and II respectively.

In each ATN, the traffic schedule consists of light, medium and heavy aircraft generated using the capacity estimation module and then converted into a traffic scenario by the evolutionary optimisation method. Figure 12 presents the maximum attainable flows in the test ARNs over a period of 24 hours.

As, for a given flow, there will be many solutions because of the combination of light, medium and heavy aircraft, we generate 20 traffic scenarios in every case. In our experiments, we control the flow by the extra separation parameter (es). Tables 6 and 7 summarise the average hourly traffic densities (hourly flight movements) for test networks ATN-I and ATN-II respectively. Their maximum hourly traffic flows (capacity) are found to be identical while the small-world configuration (ATN-II) can accommodate higher traffic than its random counterpart (ATN-I).

Table 4: ATN-I link's distance and number of way points

Links	Distance (NM)	Way points	Links	Distance (NM)	Way points	Links	Distance (NM)	Way points	Links	Distance (NM)	Way points
0 , 14	341.43	6	5 , 2	154.92	3	10 , 7	537.71	8	13 , 11	176.72	3
0 , 16	225.46	3	5 , 11	565.58	7	10 , 8	417.47	4	15 , 4	100.51	2
1 , 0	628.55	6	6 , 7	333.96	5	11 , 0	323.68	4	15 , 9	219.56	5
1 , 4	547.41	7	6 , 11	503.38	6	11 , 4	405.45	5	16 , 3	694.39	10
1 , 18	702.30	8	6 , 18	552.33	7	11 , 5	565.58	7	16 , 4	367.65	4
2 , 7	334.18	6	7 , 5	198.86	4	11 , 10	325.18	3	16 , 6	439.81	6
2 , 8	583.37	9	7 , 12	203.75	3	11 , 14	255.60	5	16 , 14	360.83	5
2 , 9	518.58	9	7 , 14	184.96	3	11 , 18	103.41	2	16 , 17	587.00	8
2 , 13	511.75	8	8 , 15	257.21	4	12 , 1	297.97	4	18 , 4	457.41	5
3 , 5	285.63	4	9 , 2	518.58	9	12 , 3	298.52	4	18 , 5	617.53	7
3 , 13	415.10	7	9 , 3	646.48	7	12 , 9	462.20	5	18 , 7	483.68	6
4 , 8	344.00	4	9 , 4	240.89	5	12 , 16	434.96	5	18 , 11	103.41	2
4 , 11	405.45	5	9 , 10	167.77	4	12 , 19	534.46	7	18 , 12	404.86	6
4 , 17	293.52	6	10 , 2	660.91	10	13 , 4	286.76	3	19 , 3	687.93	10
4 , 18	457.41	5	10 , 5	622.44	12	13 , 9	300.27	4	19 , 9	140.89	3

Table 5: ATN-II link's distance and number of way points

Links	Distance (NM)	Way points	Links	Distance (NM)	Way points	Links	Distance (NM)	Way points	Links	Distance (NM)	Way points
0 , 3	293.89	7	5 , 8	299.67	4	11 , 14	289.68	5	17 , 0	308.87	8
0 , 11	658.06	10	6 , 8	197.95	2	12 , 14	202.78	4	17 , 19	213.04	4
0 , 16	399.68	9	6 , 9	290.31	2	12 , 15	294.82	4	18 , 0	205.66	4
0 , 18	205.66	4	6 , 16	660.93	14	13 , 3	706.53	13	18 , 1	313.29	5
1 , 3	198.50	4	7 , 9	197.65	2	13 , 15	197.52	2	19 , 1	208.00	4
1 , 4	297.23	5	7 , 10	294.85	3	13 , 16	301.20	6	19 , 2	296.00	7
2 , 4	208.28	3	8 , 10	198.63	3	14 , 16	199.54	2			
2 , 5	327.82	5	8 , 11	299.57	5	14 , 17	293.17	4			
2 , 9	595.49	11	9 , 2	595.49	11	15 , 17	197.73	4			
3 , 5	216.73	4	9 , 11	202.15	5	15 , 18	296.33	5			
3 , 6	317.29	5	9 , 12	307.30	6	16 , 0	399.68	9			
3 , 13	706.53	13	10 , 11	101.59	3	16 , 6	660.93	14			
4 , 6	209.94	4	10 , 12	206.74	4	16 , 14	199.54	2			
4 , 7	308.81	5	11 , 0	658.06	10	16 , 18	198.25	4			
5 , 7	200.74	4	11 , 10	101.59	3	16 , 19	303.84	5			

For a given flow the output from the capacity estimation module is converted to a traffic scenario by a DE process, with the purpose of assigning flight levels for each that minimise the overall collision risk, while the speed and other parameters are set by ATOMS. Figure 13 shows the percentages of usage of each flight level averaged over 20 scenarios determined by calculating the total number of flight flows through a scenario divided by the total

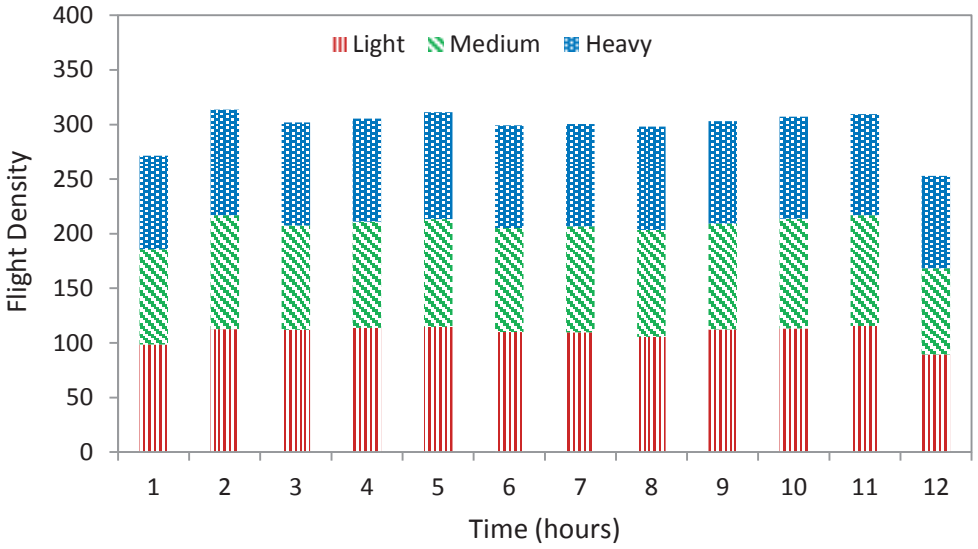

(a) Test ATN-I

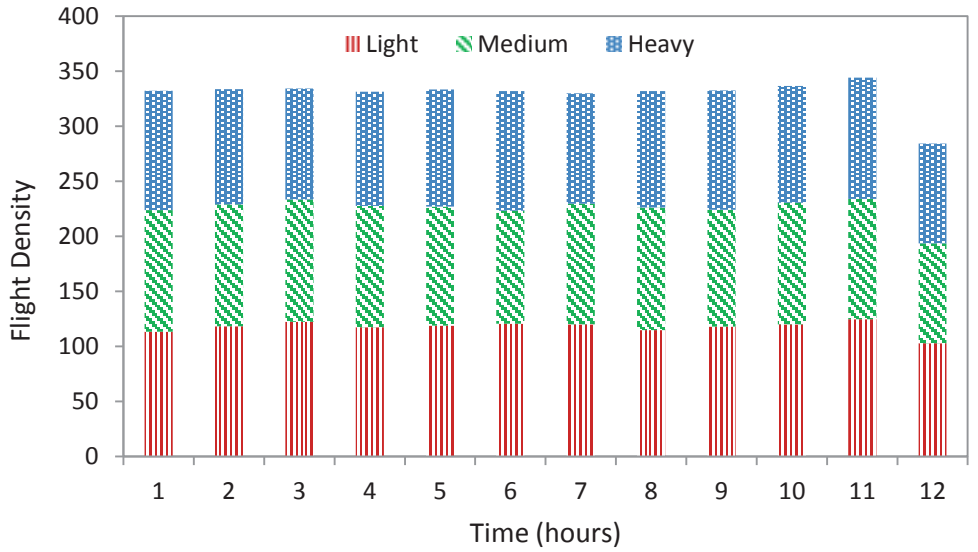

(b) Test ATN-II

Figure 12: Hourly flow of test ATNs for $es = 0$)

Table 6: Hourly flight movements in the test ARN I

es	flow	L	M	H
1	325.10 ± 6.04	131.00 ± 7.25	115.80 ± 6.79	109.55 ± 6.45
2	246.50 ± 3.99	95.00 ± 5.24	88.15 ± 5.91	87.10 ± 7.19
4	166.65 ± 3.13	64.80 ± 4.44	62.90 ± 4.81	61.55 ± 3.85
6	125.10 ± 3.18	50.60 ± 3.22	47.55 ± 3.83	46.85 ± 2.70
8	100.20 ± 3.09	40.80 ± 3.64	38.00 ± 3.31	38.05 ± 3.12
10	83.70 ± 2.30	34.00 ± 2.75	32.30 ± 2.99	32.95 ± 3.33
12	71.65 ± 2.81	30.30 ± 2.54	28.00 ± 3.21	27.05 ± 1.79
14	62.70 ± 2.72	26.95 ± 2.31	23.65 ± 3.00	25.40 ± 2.54
16	54.60 ± 2.16	24.25 ± 2.73	21.50 ± 2.26	21.00 ± 2.66
18	50.05 ± 1.85	22.50 ± 1.99	20.20 ± 2.88	19.65 ± 2.50
20	44.90 ± 1.68	20.40 ± 2.56	18.10 ± 2.13	16.90 ± 2.05

Table 7: Hourly flight movements in the test ARN II

es	flow	L	M	H
1	348.00 ± 3.67	135.70 ± 7.43	125.00 ± 6.62	121.80 ± 6.09
2	265.45 ± 3.99	102.45 ± 6.00	99.65 ± 5.43	93.55 ± 3.73
4	177.50 ± 2.96	70.05 ± 3.32	67.70 ± 4.24	65.35 ± 3.92
6	134.90 ± 2.95	53.50 ± 3.55	53.05 ± 5.41	50.85 ± 4.06
8	108.65 ± 2.37	47.90 ± 4.47	43.10 ± 4.12	42.80 ± 3.78
10	90.30 ± 1.89	38.70 ± 4.35	34.80 ± 2.44	36.15 ± 4.26
12	78.70 ± 2.03	34.30 ± 3.80	31.70 ± 3.63	31.50 ± 3.07
14	69.10 ± 1.45	31.35 ± 3.48	28.30 ± 3.16	29.35 ± 2.92
16	61.20 ± 1.15	27.60 ± 3.17	24.80 ± 2.12	25.85 ± 2.32
18	54.90 ± 1.80	25.55 ± 3.35	22.75 ± 3.11	22.15 ± 2.35
20	50.45 ± 1.54	24.05 ± 2.74	20.75 ± 2.88	20.45 ± 2.28

number of flights in it. It is clear that all the flight levels are almost equally utilised except for some traffic scenarios with es = 18 in which flight levels FL 290 and FL390 are the most used in ATN-I and ATN-II respectively.

Figure 14 shows the collision risk of each test ATN as a function of the hourly flow. As the number of hourly flight movements increases, all collision risks increase almost linearly for both cases, with the average collision risk always more for ATN-I than ATN-II. In both cases, the collision risk hits the TLS (1.5×10^{-8}) [18] as the hourly flight movements among the airports increase which we call the critical flow, with those of ATN-I and ATN-II 135 and 115 (hourly flight movements) respectively.

7. Conclusions

With the aim of increasing the capacity and enhancing the safety of air transportation, this paper proposed a framework for airport and airspace

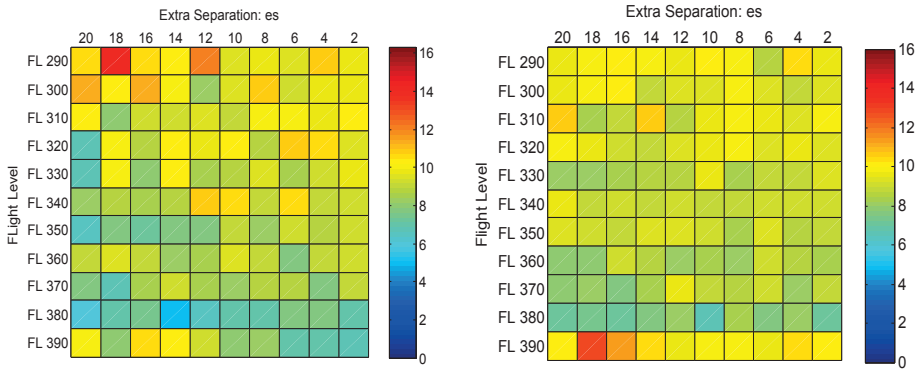

(a) Test ATN-I (b) Test ATN-II

Figure 13: Percentages of usage of different flight levels

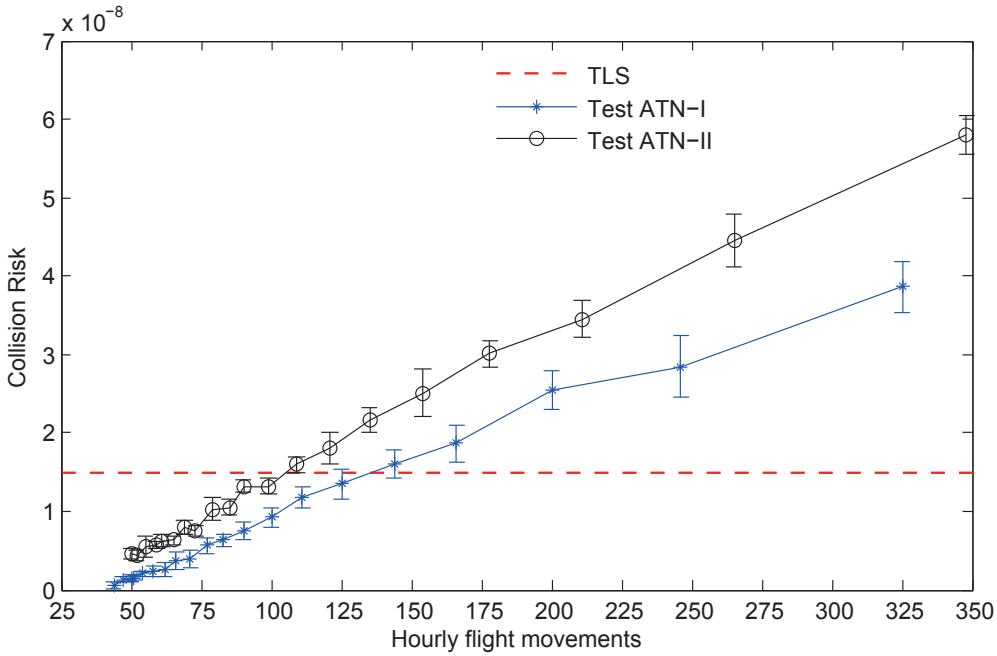

Figure 14: Capacity-Collision risk relationship

network interaction with the aim of analyzing the trade-off between capacity and safety. The proposed methodology was tested on two different ATN topologies random (ATN-I) and small-world (ATN-II) with the same number of airports.

The experimental results indicated that, if the airspace TLS was relaxed, the maximum hourly flow (capacity) of the small-world configuration (ATN-II) could accommodate more traffic than the random one (ATN-I). In both cases, as the flow increased in the airport network, the overall airspace's collision risk increased linearly and crossed the TLS because, although the airport network system could handle more traffic, the safety barrier of the airspace served as a bottleneck in terms of the overall capacity of the air traffic network. Therefore, estimating the true capacity of an air transportation network system without considering safety is very unrealistic as its maximum capacity depends on the interactions of its underlying airport network and airspace waypoints network.

It was found that, in general, the capacity upper bound depends not only on the connectivity among airports and their individual performances but also the configuration of waypoints and mid-air interactions among flights. We demonstrated that, as the hourly flow in the network increased after a certain level, the overall collision risk crossed the TLS which we defined as the critical flow for the given ATN. However, as the location of the critical point depends on the particular network configuration, it may vary from network to network. The critical flow of the random topology (ATN-I) was found to be larger than its small-world counterpart while, in terms of airspace safety, its collision risk was smaller for the same flight. These results may facilitate decision-makers in gaining insights into how capacity and safety interact with each other, discovering system bottlenecks and using such knowledge to improve an ATN's performance and sustainability.

References

[1] Ahmed, M.S., Alam, S., 2016. An evolutionary optimization approach to maximize runway throughput capacity for hub and spoke airports, in: Australasian Conference on Artificial Life and Computational Intelligence, Springer. pp. 313–323.

[2] Alam, S., Abbass, H., Barlow, M., et al., 2008. ATOMS: Air traffic operations and management simulator. IEEE Transactions on Intelligent Transportation Systems 9, 209–225.

[3] Alam, S., Hossain, M.M., Al-Alawi, F., Al-Thawadi, F., 2015. Optimizing lateral airway offset for collision risk mitigation using differential evolution. Air Traffic Control Quarterly 23, 301–324.

[4] Alam, S., Lokan, C., Aldis, G., Barry, S., Butcher, R., Abbass, H., 2013. Systemic identification of airspace collision risk tipping points using an evolutionary multi-objective scenario-based methodology. Transportation research part C: emerging technologies 35, 57–84.

[5] Alam, S., Shafi, K., Abbass, H.A., Barlow, M., 2009. An ensemble approach for conflict detection in free flight by data mining. Transportation research part C: emerging technologies 17, 298–317.

[6] Bourke, P., 1989. Efficient triangulation algorithm suitable for terrain modelling, in: Pan Pacific Computer Conference, Beijing, China.

[7] Chen, Y., Zhang, D., 2014. Dynamic airspace configuration method based on a weighted graph model. Chinese Journal of Aeronautics 27, 903–912.

[8] Donohue, G.L., . A simplified air transportation system capacity model. Journal of Air Traffic Control , 8–15.

[9] Donohue, G.L., 2001. A macroscopic air transportation capacity model: Metrics and delay correlation, in: New Concepts and Methods in Air Traffic Management. Springer, pp. 45–62.

[10] Erdös, P., Rényi, A., 1960. On the evolution of random graphs. Publication of the Mathematical Institute of the Hungarian Academy of Sciences 5, 17–61.

[11] EUROCONTROL, 2010. Indicators and analysis of the atm network operations performance. Cenrtal Flow Management Unit, Brussels, Network Operations Report.

[12] Gilbo, E.P., 1993. Airport capacity: Representation, estimation, optimization. IEEE Transactions on Control Systems Technology 1, 144–154.

[13] Graham, R., Young, D., 2006. Preparing an initial assessment of the SESAR concept of operations ?EP3: Single european sky implementation support through validation? Technical Report. Technical report, Eurocontrol Experimental Centre, France.

[14] Haynie, R.C., 2002. An investigation of capacity and safety in near-terminal airspace for guiding information technology adoption.

[15] Hossain, M., Alam, S., Abbass, H., 2015. A dynamic multi-commodity flow optimization algorithm for estimating airport network capacity, in: ENRI International Workshop on ATM/CNS, Tokyo, Japan.

[16] Hossain, M., Alam, S., Rees, T., Abbass, H., 2013. Australian airport network robustness analysis: a complex network approach, in: Australasian Transport Research Forum (ATRF), 36th, 2013, Brisbane, Queensland, Australia.

[17] Hsu, D., 1981. The evaluation of aircraft collision probabilities at intersecting air routes. Journal of Navigation 34, 78–102.

[18] ICAO, 1995. Review of the General Concept of Separation Panel. Technical Report. Working Group A Meeting: Summary of Discussion and Conclusions.

[19] ICAO, 2008. Unified framework for collision risk modelling in support of the manual on airspace planning methodology with further applications, circ 319-an/181 ed. International Civil Aviation Organization, Montreal, Canada .

[20] Jacquillat, A., Odoni, A.R., 2017. A new airport demand management approach based on targeted scheduling interventions. Journal of Transport Economics and Policy (JTEP) 51, 115–138.

[21] Kai-Quan, C., Jun, Z., Wen-Bo, D., Xian-Bin, C., 2012. Analysis of the chinese air route network as a complex network. Chinese Physics B 21, 028903.

[22] Kopardekar, P., Bilimoria, K.D., Sridhar, B., 2008a. Airspace configuration concepts for the next generation air transportation system. Air Traffic Control Quarterly 16.

[23] Kopardekar, P., Rhodes, J., Schwartz, A., Magyarits, S., Willems, B., 2008b. Relationship of maximum manageable air traffic control complexity and sector capacity, in: 26th International Congress of the Aeronautical Sciences (ICAS 2008), and AIAA-ATIO-2008-8885, Anchorage, Alaska, Sept, pp. 15–19.

[24] Lin, X., Fulton, N., Westcott, M., 2009. Target level of safety measures in air transportation–review, validation and recommendations, in: Proceedings of the IASTED International Conference, p. 222.

[25] McNally, D., Thipphavong, D., 2008. Automated separation assurance in the presence of uncertainty, in: Proc 26th International Congress of the Aeronautical Sciences.

[26] Mehadhebi, K., 2000. A methodology for the design of a route network, in: Proceedings of the Third Air Traffic Management R & D Seminar ATM-2000, pp. 8–69.

[27] Netjasov, F., 2012. Framework for airspace planning and design based on conflict risk assessment: Part 1: Conflict risk assessment model for airspace strategic planning. Transportation research part C: emerging technologies 24, 190–212.

[28] Perrottet, J., 2017. Performance based navigation, in: Integrated Communications, Navigation and Surveillance Conference (ICNS), 2017, IEEE. pp. 1–9.

[29] Pesic, B., Durand, N., Alliot, J.M., 2001. Aircraft ground traffic optimisation using a genetic algorithm, in: GECCO 2001, Genetic and Evolutionary Computation Conference.

[30] Planning, J., 2007. Development office: Concept of operations for the next generation air transportation system. Draft Version 0.2 (July 24, 2006) .

[31] Price, K., Storn, R.M., Lampinen, J.A., 2006. Differential evolution: a practical approach to global optimization. Springer Science & Business Media.

[32] Pyrgiotis, N., Odoni, A., 2015. On the impact of scheduling limits: A case study at newark liberty international airport. Transportation Science 50, 150–165.

[33] Sheridan, T.B., 2006. Next generation air transportation systems: Human-automation interaction and organizational risks, in: Proceedings of the 2nd Symposium on Resilience Engineering, pp. 272–282.

[34] Stroeve, S.H., Blom, H.A., Bakker, G.B., 2009. Systemic accident risk assessment in air traffic by monte carlo simulation. Safety science 47, 238–249.

[35] Symon, F., Alam, S., Hossain, M.M., Blom, H., . Airspace network characterization for effect of intermediate waypoints on collision risk assesment .

[36] Watts, D.J., Strogatz, S.H., 1998. Collective dynamics of small-worldnetworks. nature 393, 440–442.

[37] Wenjing, Z., Richard, C., Abbass, H., 2015. Dynamic capacity-demand balance in air transport systems using co-evolutionary computational red teaming, in: Proceeding of the 5th International Air Transport and Operations Symposium.

[38] Ye, B., Hu, M., Shortle, J.F., 2014. Collision risk-capacity tradeoff analysis of an en-route corridor model. Chinese Journal of Aeronautics 27, 124–135.

[39] Yousefi, A., Xie, R., 2011. Safety-capacity trade-off and phase transition analysis of automated separation assurance concepts, in: 30th IEEE/AIAA Digital Avionics Systems Conference (DASC), IEEE. pp. 1B5–1.

[40] Zhang, X., Guan, X., Zhu, Y., Lei, J., 2015. Strategic flight assignment approach based on multi-objective parallel evolution algorithm with dynamic migration interval. Chinese Journal of Aeronautics 28, 556–563.